

Supporting Information

Bio-Based Palladium Catalyst in Cryogel for Cross-Coupling Reactions

Elisabetta Grazia Tomarchio,^{a,b} Chiara Zagni,*^a Vincenzo Paratore,^c Guglielmo Guido Condorelli,^c Sabrina Carola Carroccio,^d Antonio Rescifina^a

^aDepartment of Drug and Health Sciences, University of Catania, V.le A. Doria 6, 95125, Catania, Italy

^bDepartment of Biomedical and Biotechnological Sciences, University of Catania, Via Santa Sofia 97, 95123 Catania, Italy

^cDepartment of Chemical Science, Università degli Studi di Catania, Viale Andrea Doria 6, 95125, Catania, Italy

^dInstitute for Polymers, Composites, and Biomaterials CNR-IPCB, Via Paolo Gaifami 18, 95126, Catania, Italy

*Correspondence: chiara.zagni@unict.it (C.Z.)

Table of Contents

- 1 NMR Spectra of Pheb and PhebPd
2. Porosimetric analysis
3. EDX analysis
4. Swelling ratio
5. Characterization Data and ¹H NMR Spectra of Suzuki reaction products

1. NMR Spectra of PheB (3) and PheBPd (4)

N-(4-vinylbenzyl)phenylalanine (Pheb) (3)

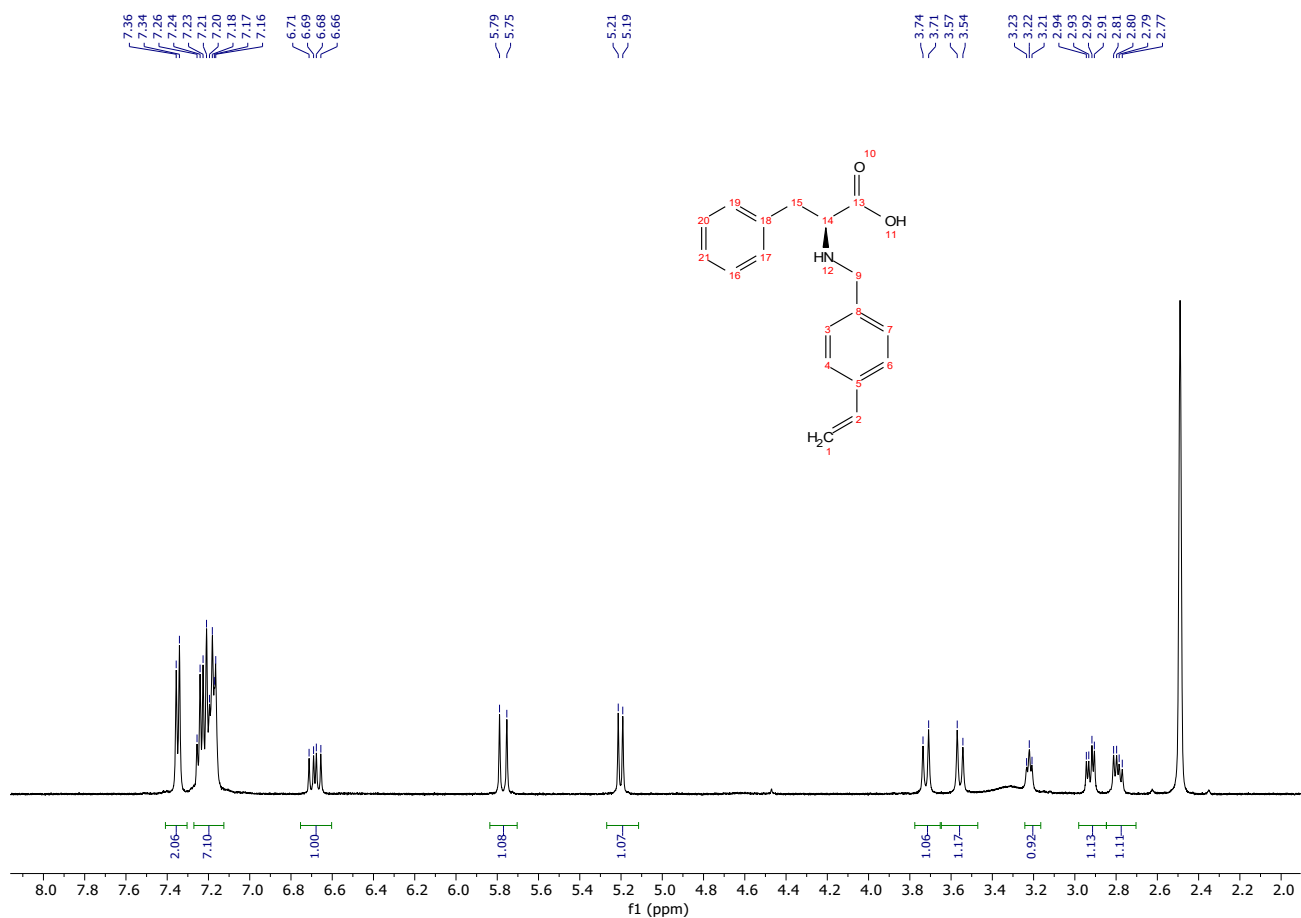


Figure S1. ¹H NMR spectrum of Pheb 3.

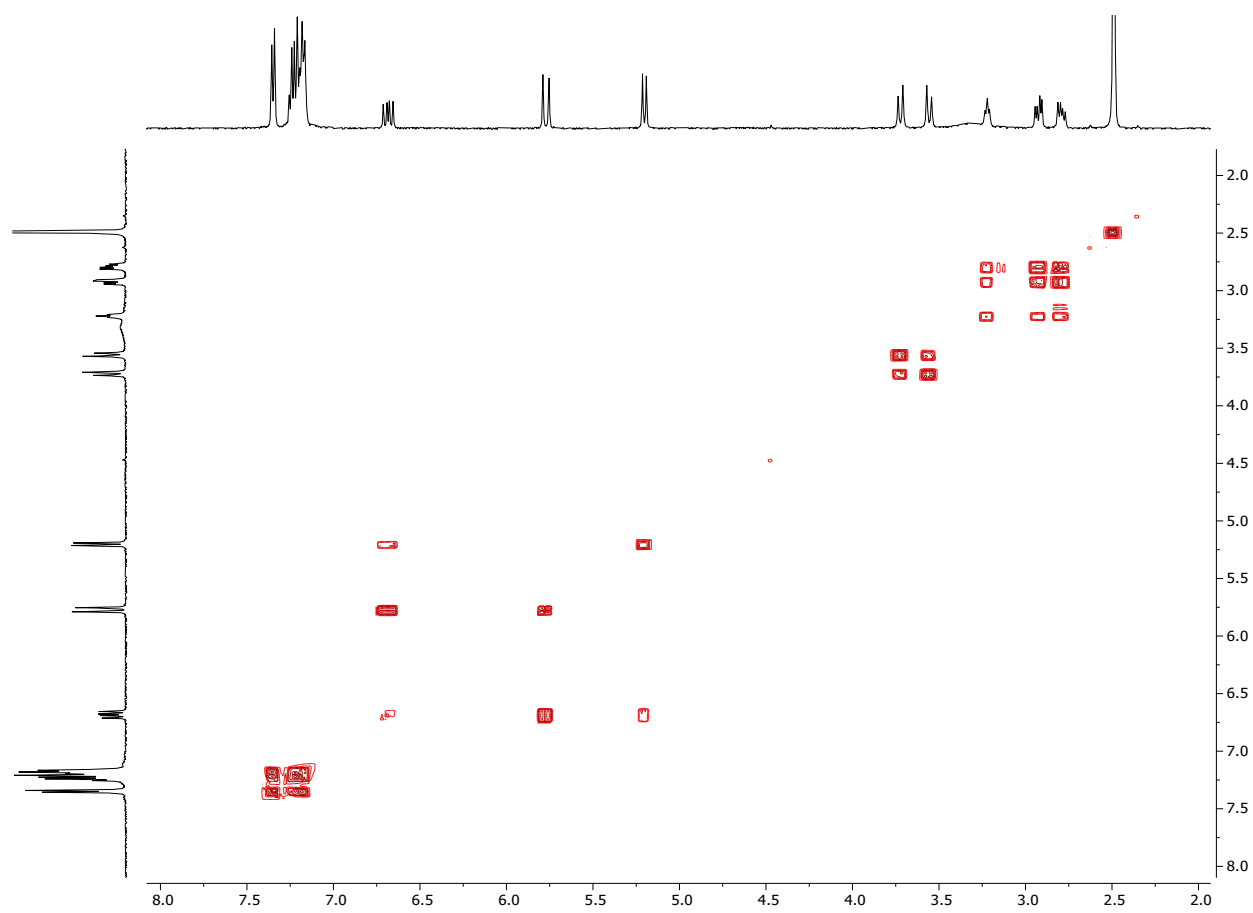


Figure S2. gCOSY spectrum of Pheb 3.

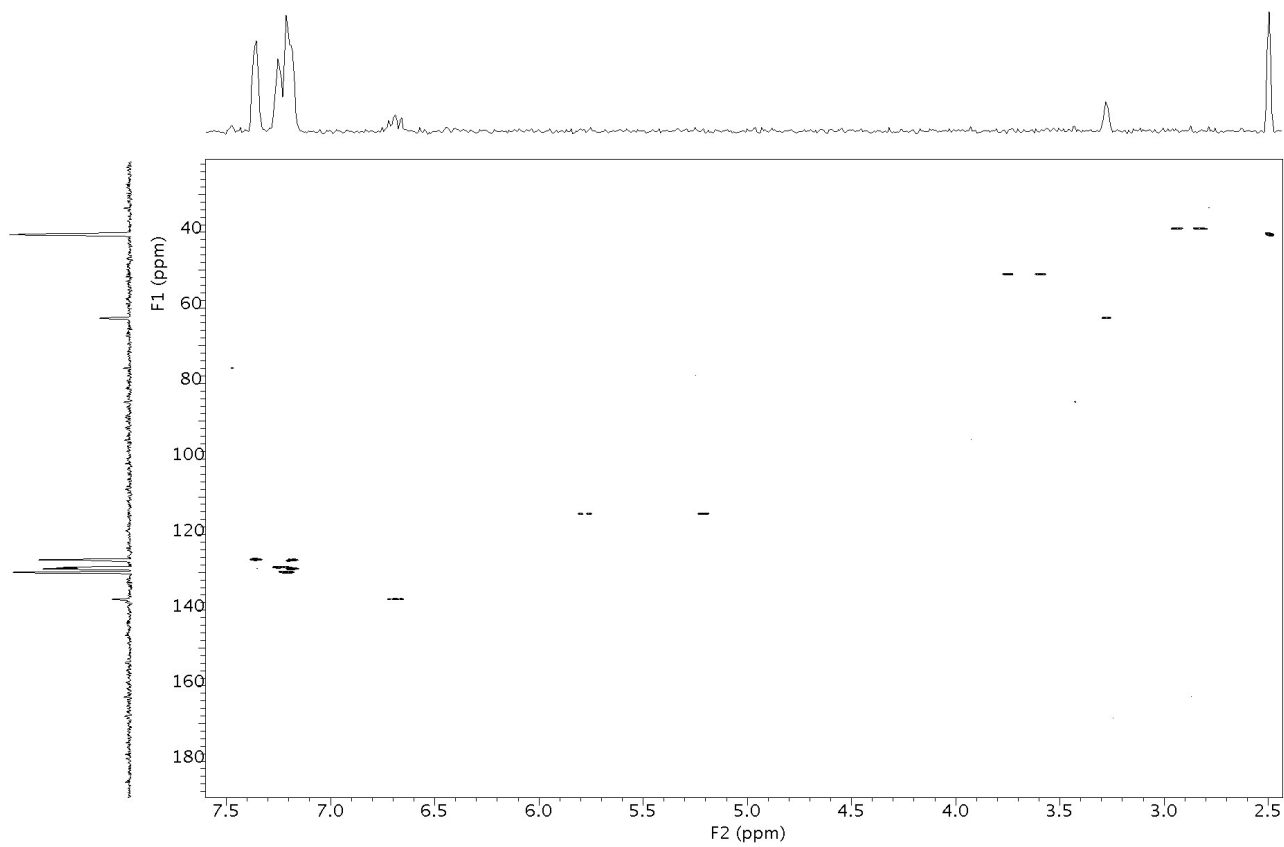


Figure S3. gHSQC spectrum of Pheb 3

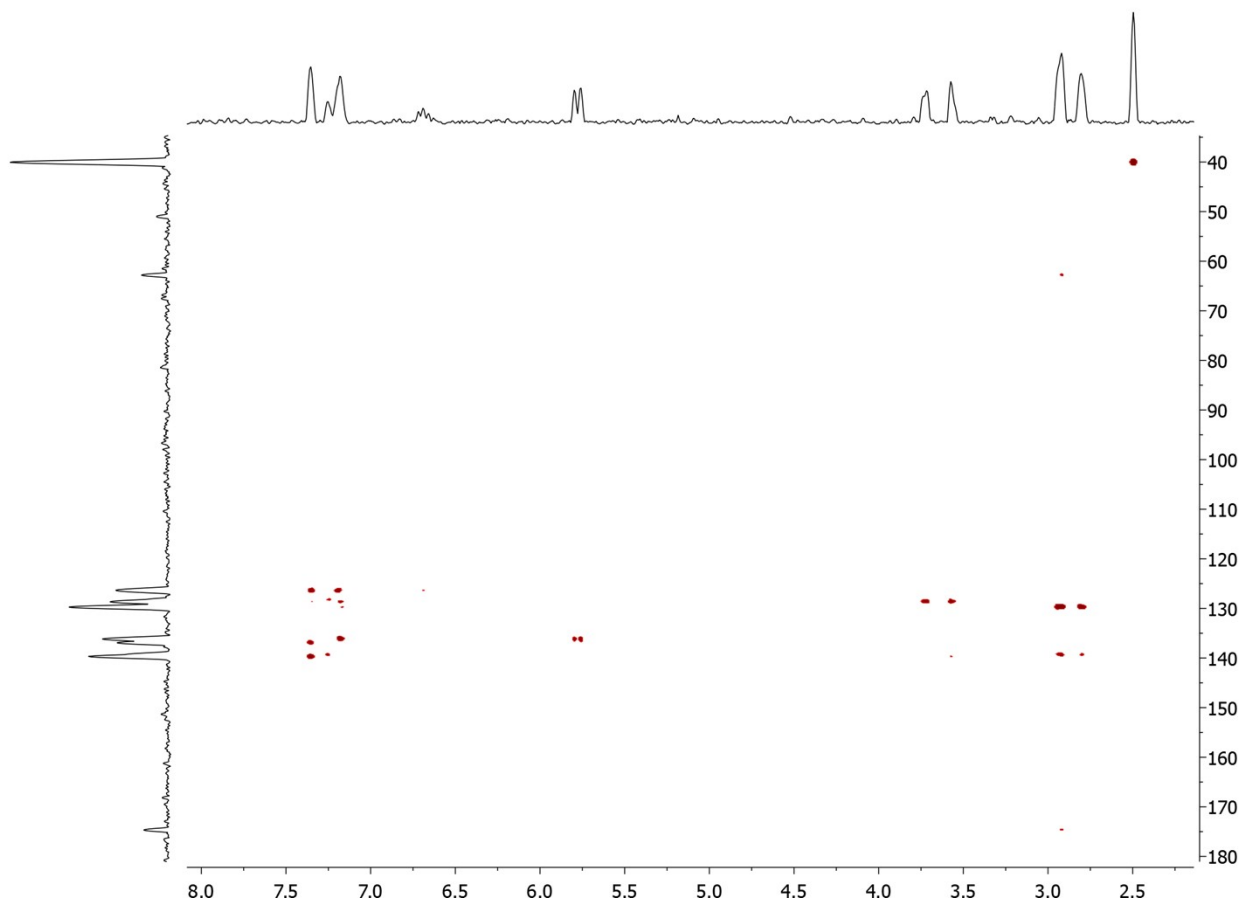


Figure S4. gHMBC spectrum of Pheb **3**

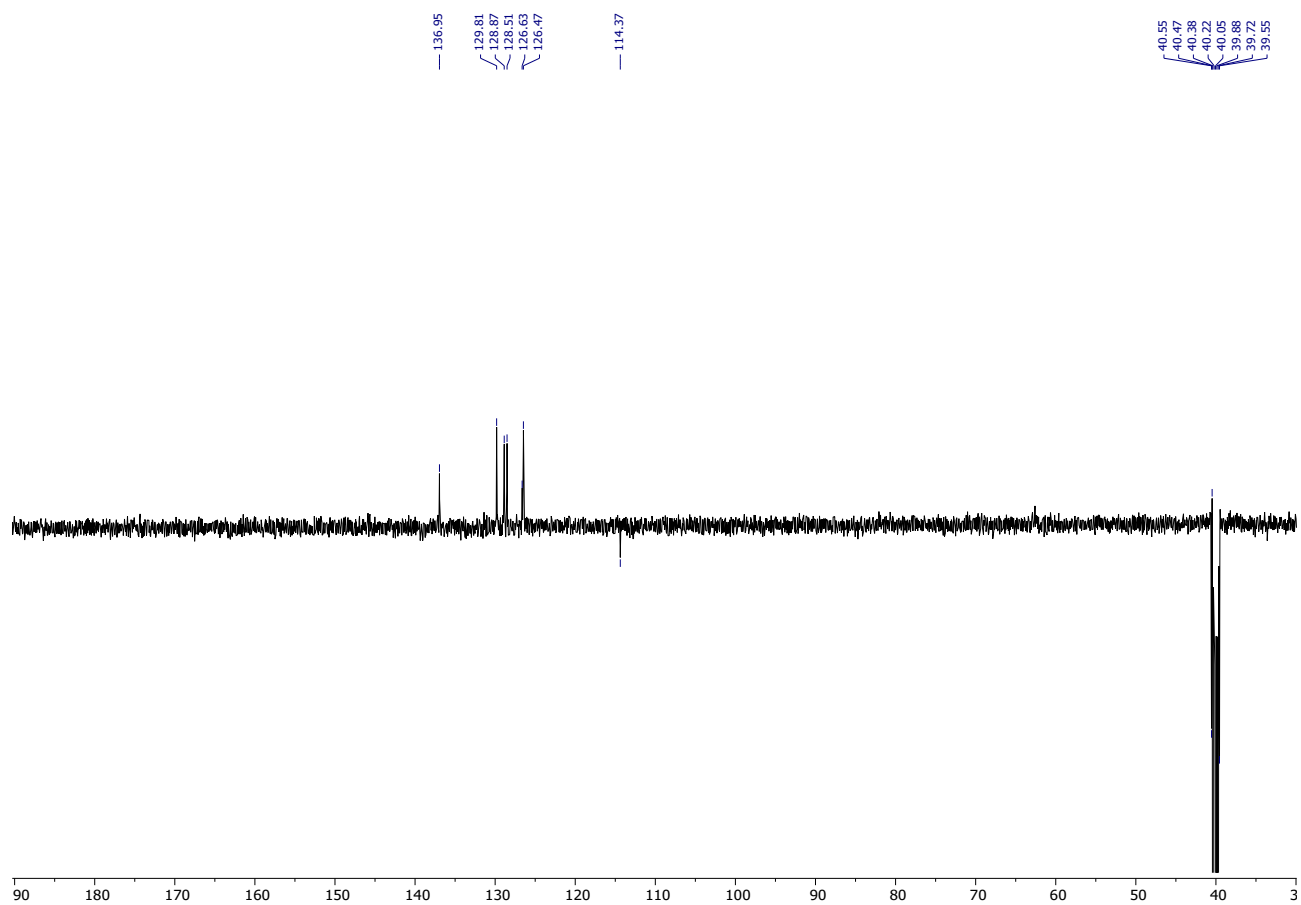


Figure S5. APT spectrum of Pheb 3

Bis-[*N*-(4-vinylbenzyl)phenylalanine]palladium(II) complex (PhebPd) (4)

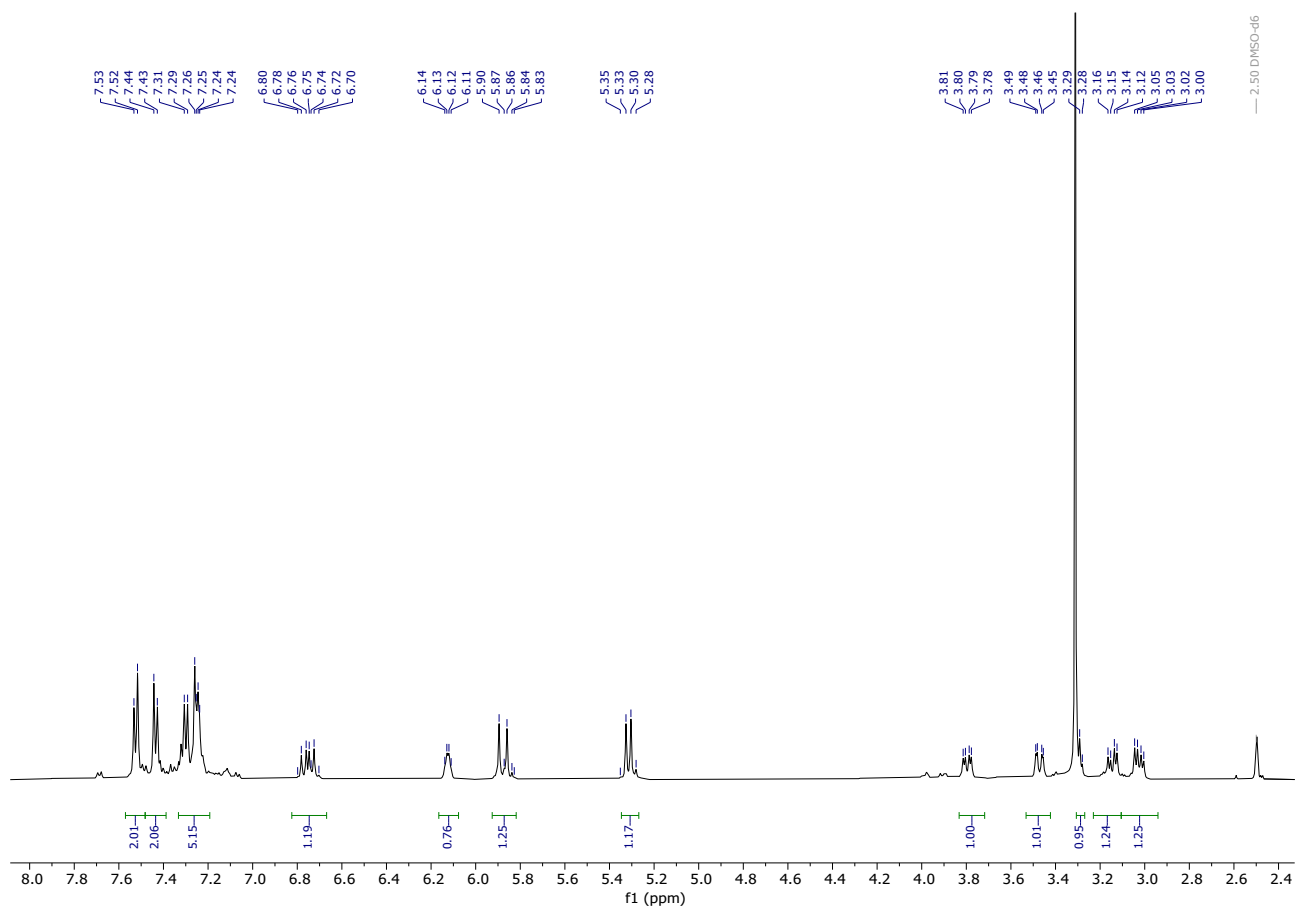


Figure S6. ^1H NMR spectrum of PhebPd **4**.

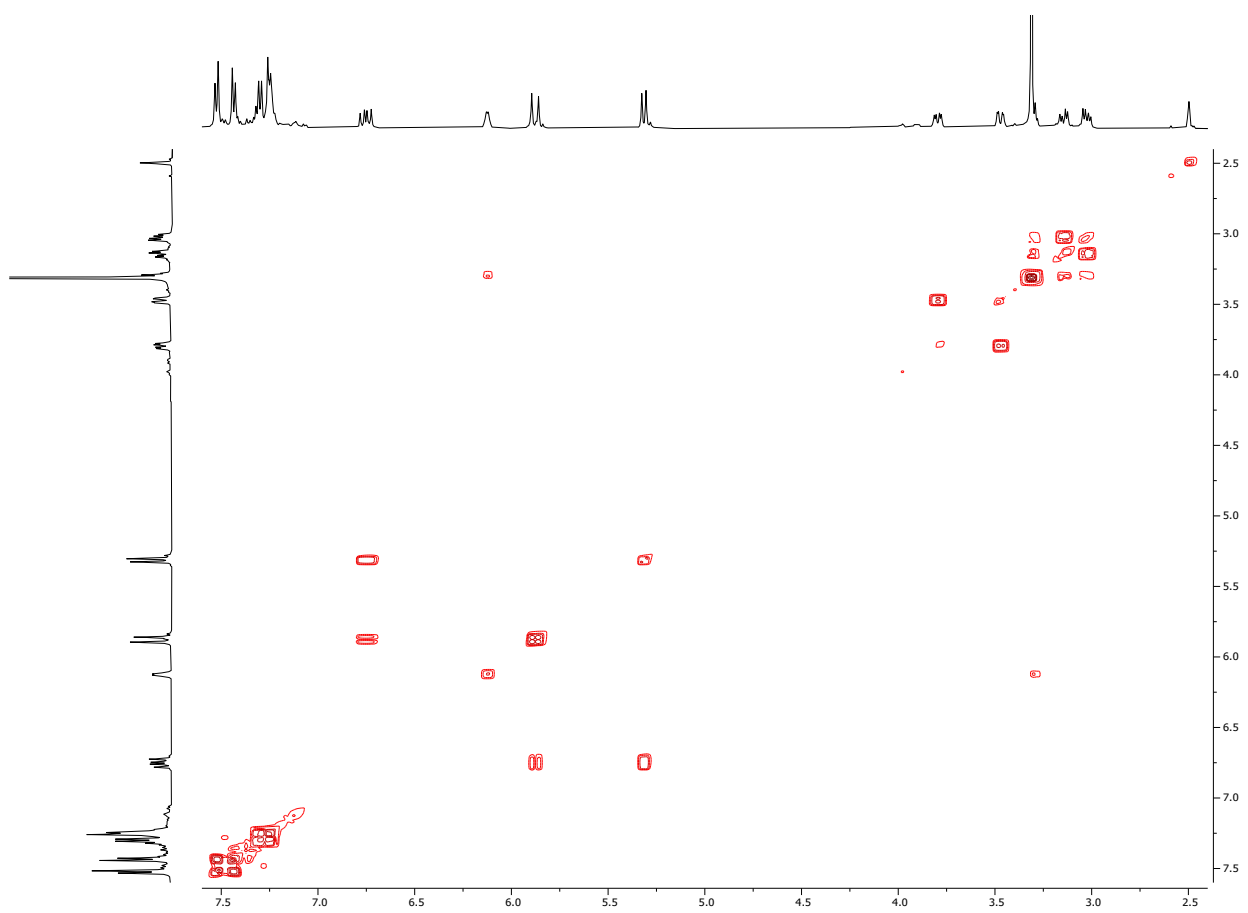


Figure S7. gCOSY spectrum of PhebPd 4.

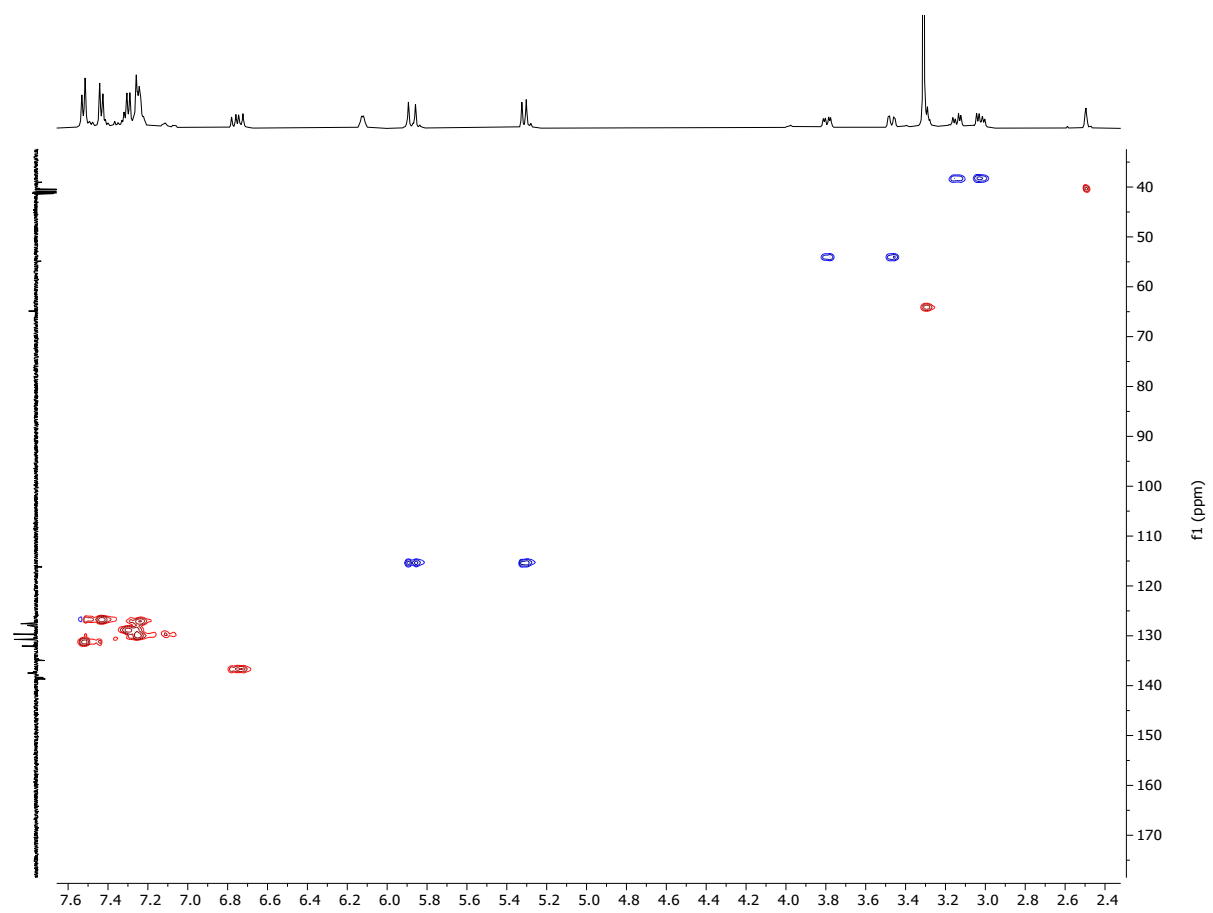


Figure S8. gHSQC spectrum of PhebPd 4.

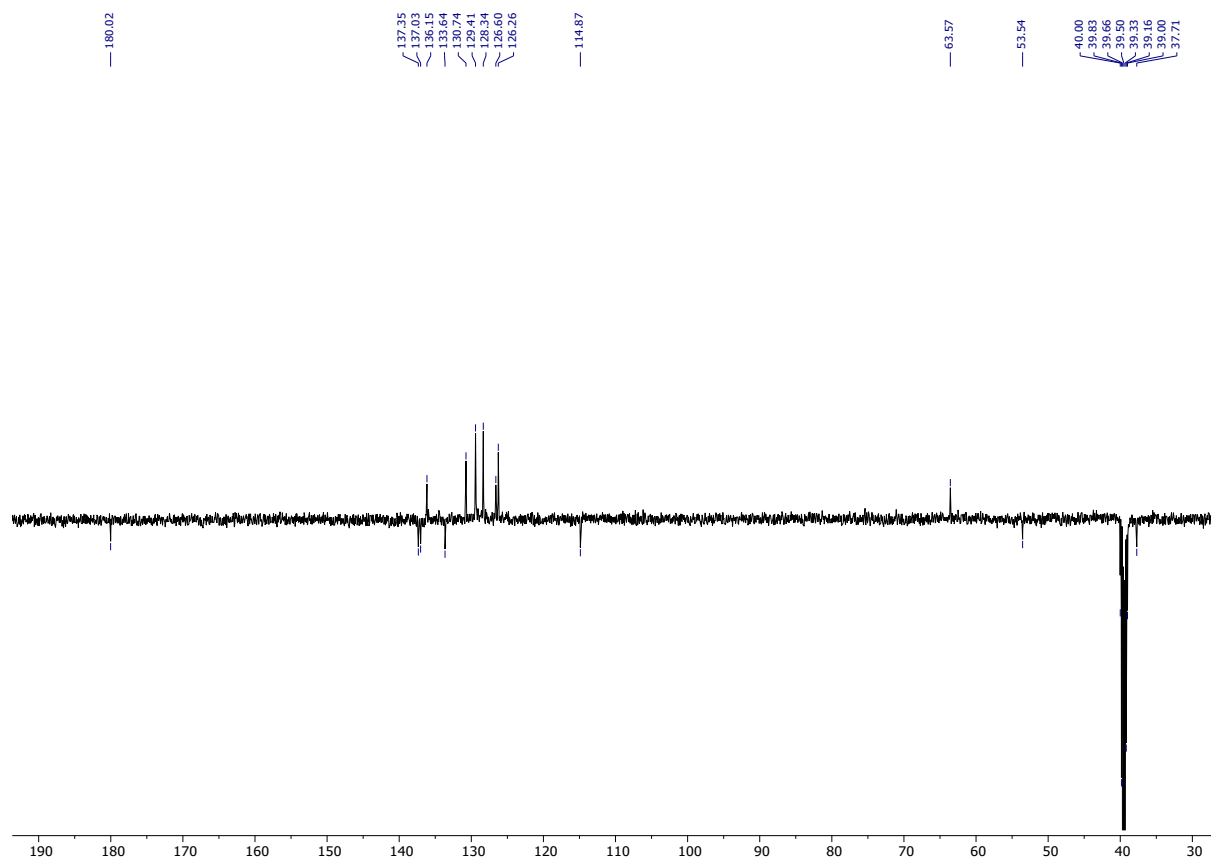


Figure S9. APT spectrum of PhebPd 4.

2. Porosimetric analysis

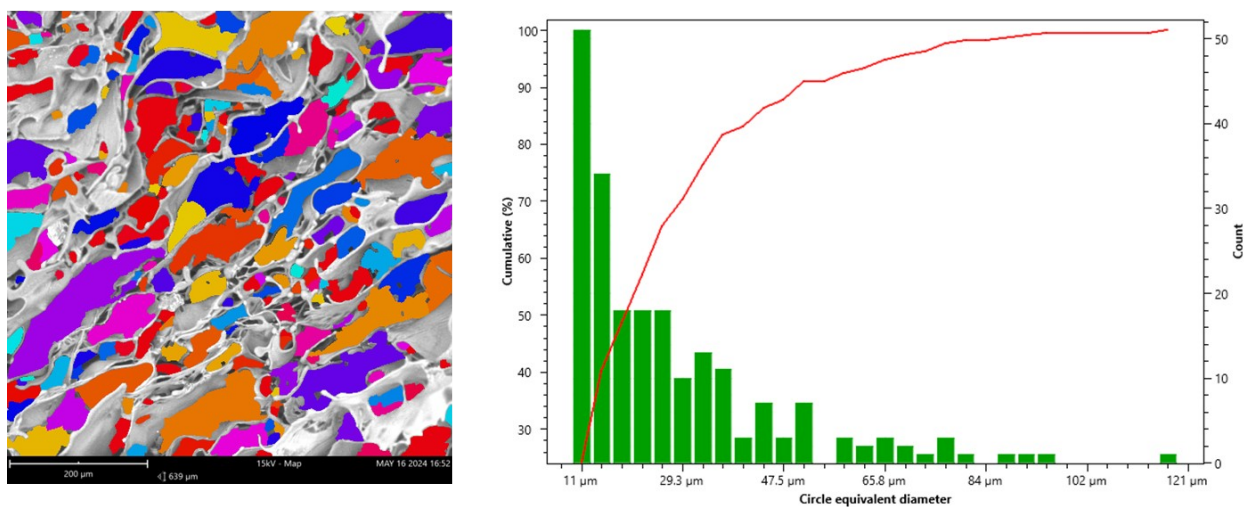


Figure S10. Porosimetric distribution of C-PhebPd.

Table S1.

Property	Median	Average
Circle equivalent diameter	22.7 μm	28.7 μm
Major axis	29.9 μm	41.6 μm
Minor axis	16 μm	20.4 μm
Circumference	88.5 μm	121 μm
Convex hull	85.1 μm	111 μm
Circumscribed circle diameter	34 μm	46.8 μm
Area	403 μm^2	927 μm^2
Volume by area	6.09 $\times 10^3$ μm^3	3.50 $\times 10^4$ μm^3

3. EDX analysis

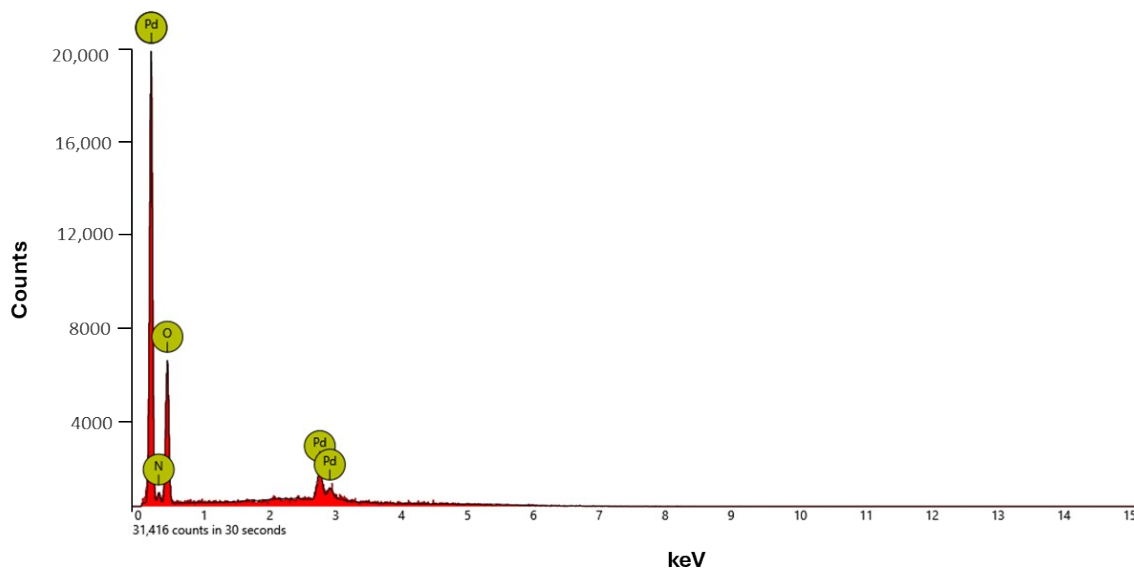


Figure S11. EDX of C-PhebPd.

4. Swelling ratio

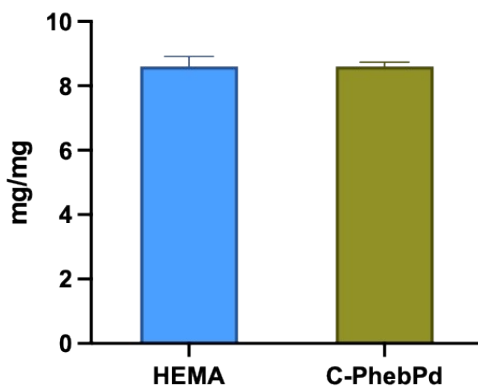


Figure S12. Swelling ratio of C-PhebPd compared with a cryogel of HEMA.

5. Characterization Data and ^1H NMR Spectra of Suzuki reaction products

[1,1'-biphenyl]-4-carbaldehyde

^1H NMR (500 MHz, CDCl_3) δ 9.91 (s, 1H), 7.81 (d, $J = 7.8$ Hz, 2H), 7.61 (d, $J = 7.9$ Hz, 2H), 7.49 (d, $J = 7.5$ Hz, 2H), 7.34 (t, $J = 7.6$ Hz, 2H), 7.31–7.26 (m, 1H).

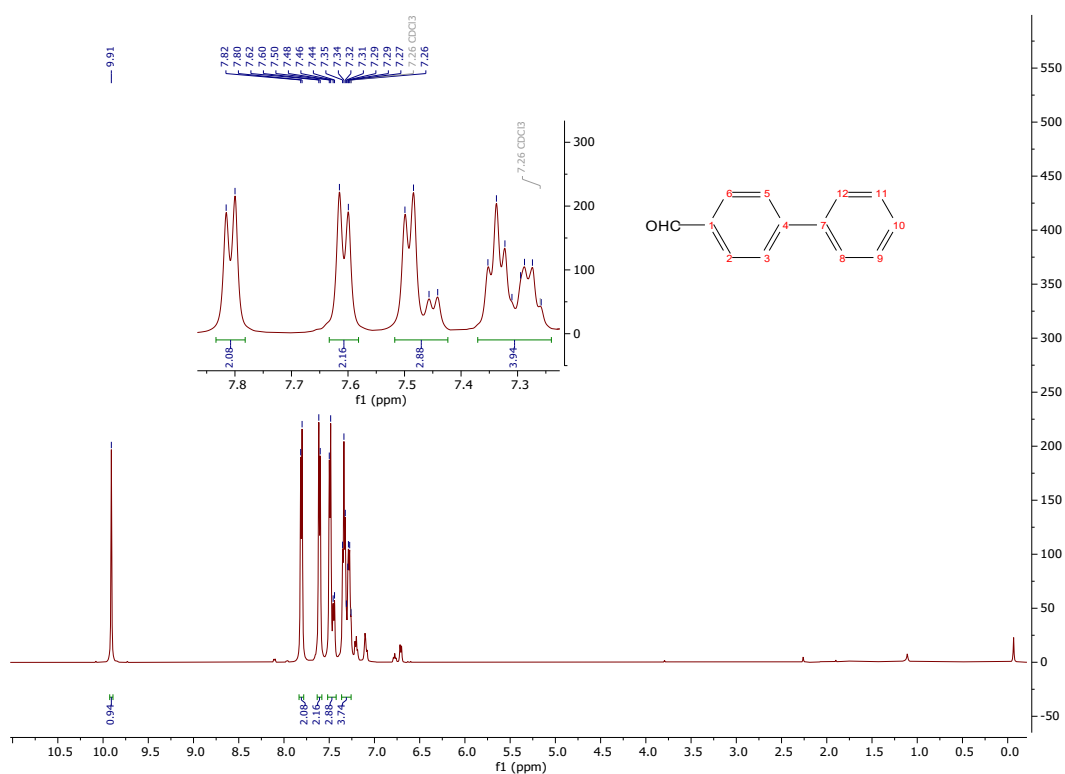


Figure S13. ^1H NMR of [1,1'-biphenyl]-4-carbaldehyde.

1,1'-biphenyl

^1H NMR (500 MHz, CDCl_3) δ 7.60 (d, $J = 7.5$ Hz, 2H), 7.45 (t, $J = 7.6$ Hz, 2H), 7.35 (t, $J = 7.4$ Hz, 1H)

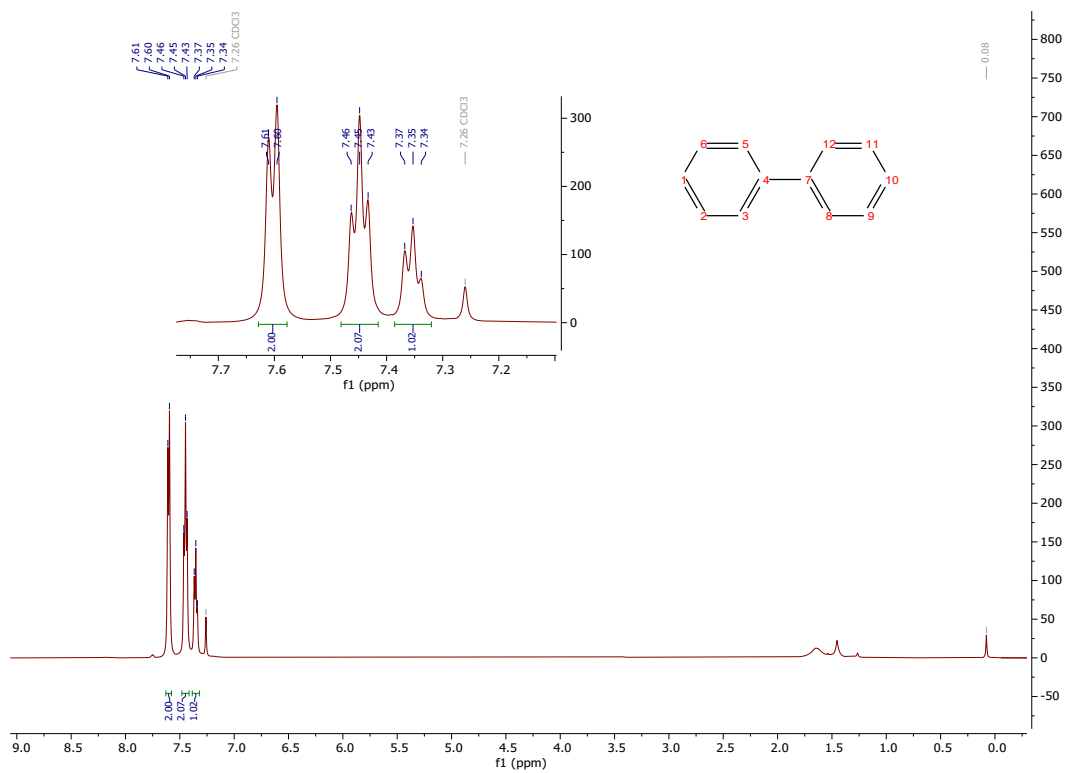


Figure S14. ^1H NMR of 1,1'-biphenyl.

2-(4-methoxyphenyl)furan

^1H NMR (500 MHz, CDCl_3) δ 7.61 (d, $J = 8.3$ Hz, 2H), 7.43 (s, 1H), 6.92 (d, $J = 8.3$ Hz, 2H), 6.51 (d, $J = 3.3$ Hz, 1H), 6.45 (d, $J = 3.3$ Hz, 1H), 3.84 (s, 3H).

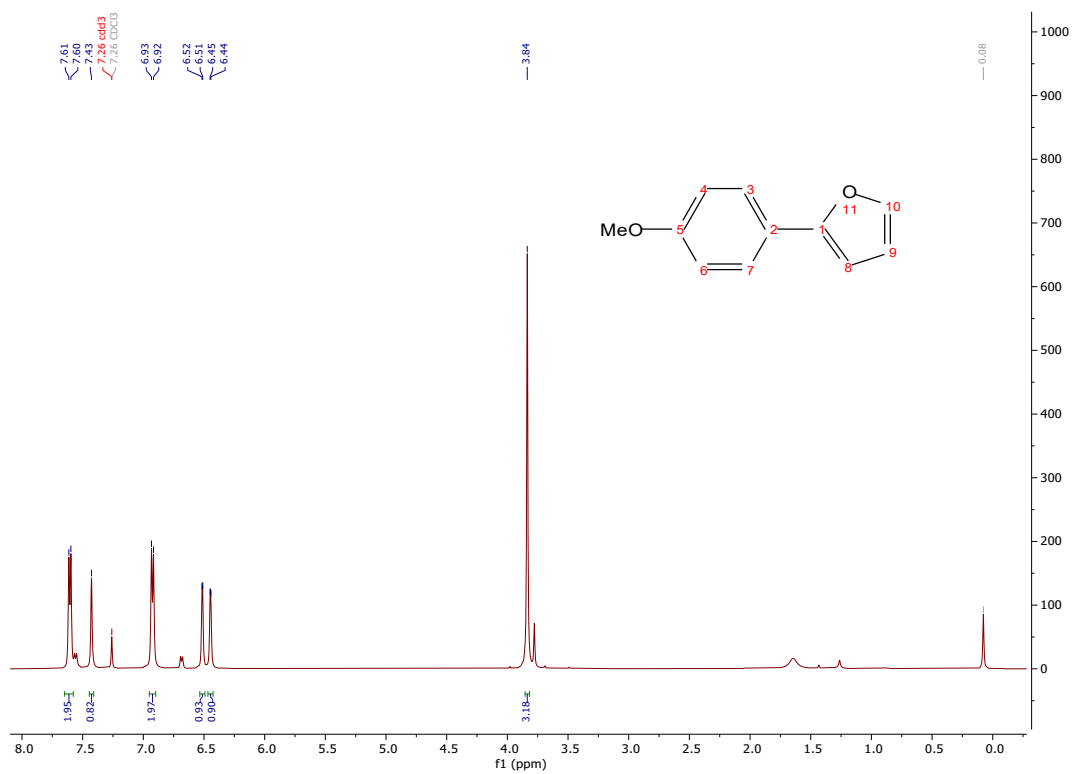


Figure S15. ^1H NMR of 2-(4-methoxyphenyl)furan.

2-(4-methoxyphenyl)thiophene

^1H NMR (500 MHz, CDCl_3) δ 7.55 (d, $J = 8.2$ Hz, 2H), 7.21 (dd, $J = 7.3, 4.3$ Hz, 2H), 7.06 (t, $J = 4.4$ Hz, 1H), 6.92 (d, $J = 8.2$ Hz, 2H), 3.84 (s, 3H).

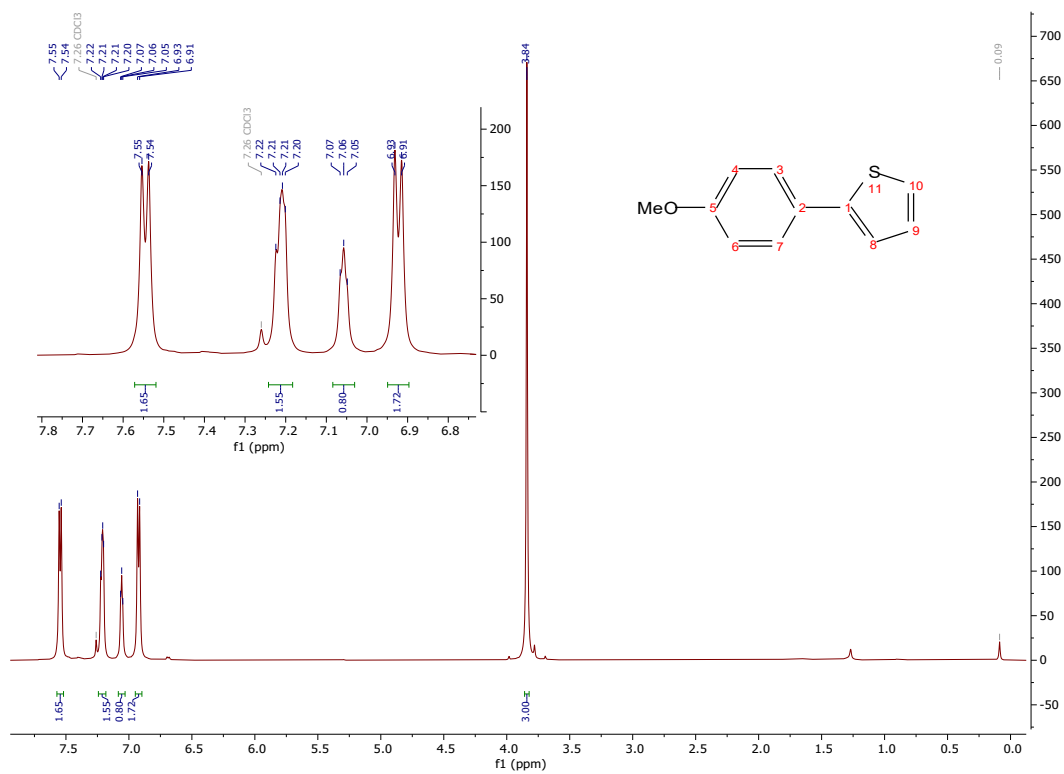


Figure S16. ^1H NMR of 2-(4-methoxyphenyl)thiophene.

2-phenylfuran

^1H NMR (500 MHz, CDCl_3) δ 7.60–7.54 (m, 2H), 7.36 (d, $J = 1.9$ Hz, 1H), 7.28 (t, $J = 7.6$ Hz, 2H), 7.18–7.12 (m, 1H), 6.54 (d, $J = 3.3$ Hz, 1H), 6.37 (dd, $J = 3.5, 1.8$ Hz, 1H).

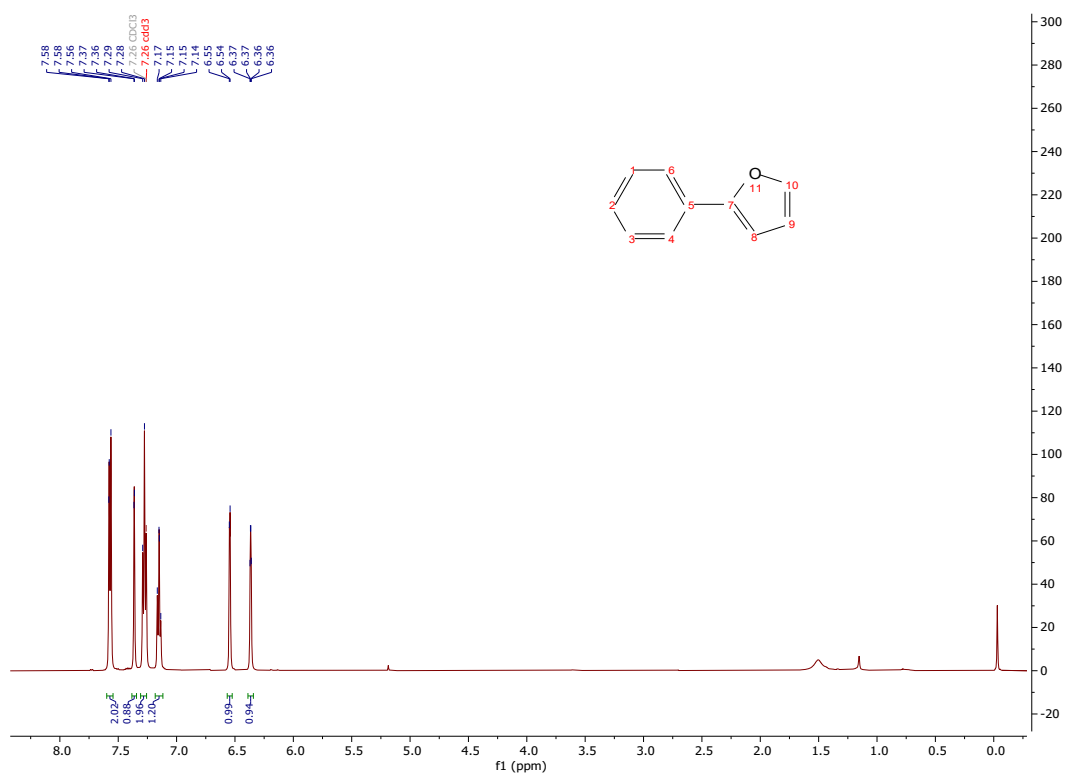


Figure S17. ^1H NMR of 2-phenylfuran.

2-phenylthiophene

^1H NMR (500 MHz, CDCl_3) δ 7.54 (d, $J = 7.7$ Hz, 2H), 7.31 (t, $J = 7.6$ Hz, 2H), 7.26–7.17 (m, 3H), 7.01 (t, $J = 4.3$ Hz, 1H).

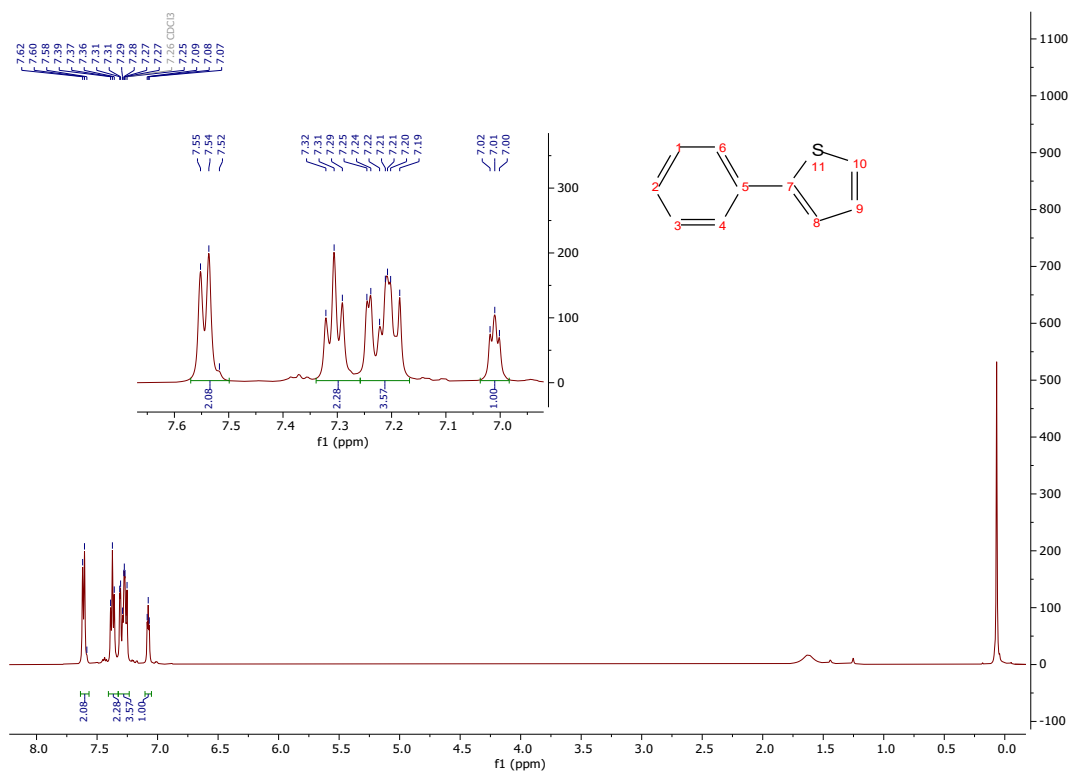


Figure S18. ^1H NMR of 2-phenylthiophene.

2,4-dimethoxy-5-phenylpyrimidine

^1H NMR (500 MHz, CDCl_3) δ 8.26 (s, 1H), 7.49 (d, $J = 7.6$ Hz, 2H), 7.43 (t, $J = 7.6$ Hz, 2H), 7.37 (d, $J = 7.3$ Hz, 1H), 4.04 (d, $J = 9.1$ Hz, 6H).

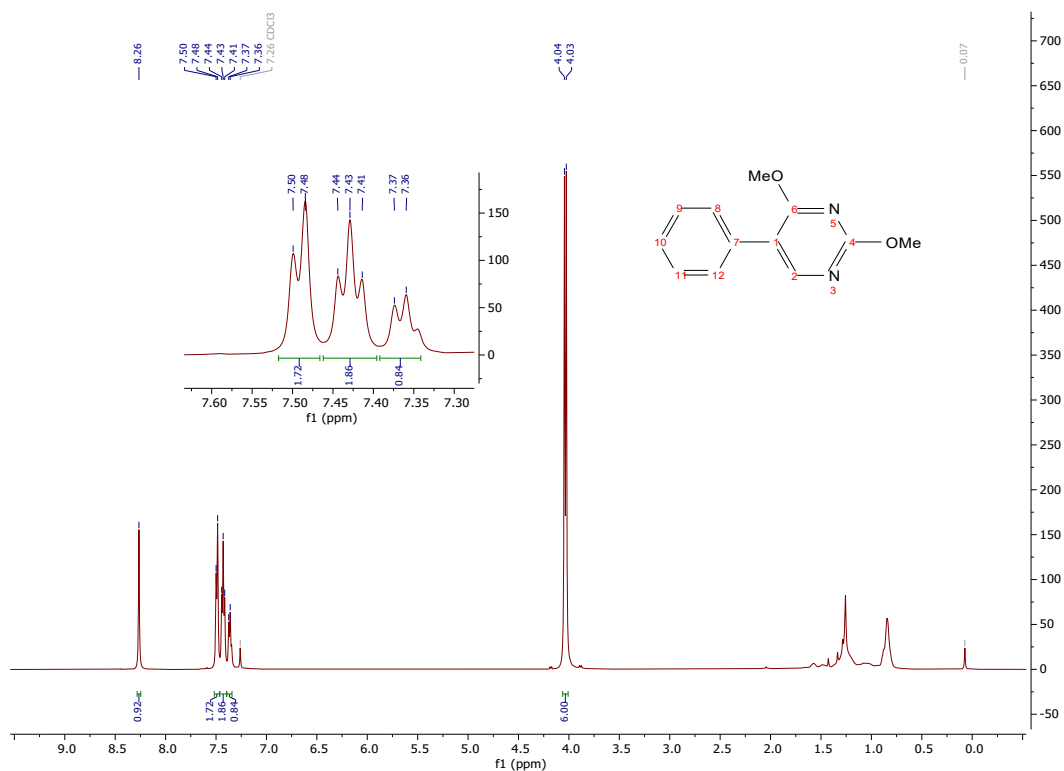


Figure S19. ^1H NMR of 2,4-dimethoxy-5-phenylpyrimidine.

4-(furan-2-yl)benzaldehyde

^1H NMR (500 MHz, CDCl_3) δ 9.99 (s, 1H), 7.90 (d, $J = 8.0$ Hz, 2H), 7.82 (d, $J = 8.0$ Hz, 2H), 7.55 (s, 1H), 6.85 (d, $J = 3.5$ Hz, 1H), 6.53 (d, $J = 2.6$ Hz, 1H).

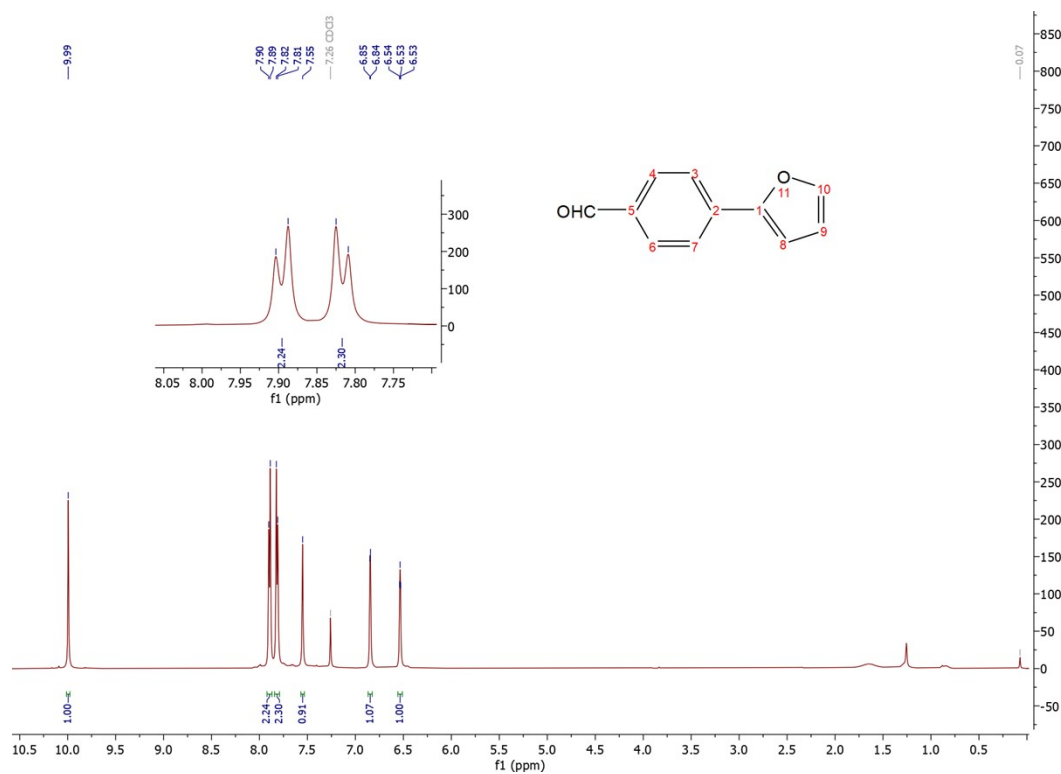


Figure S20. ^1H NMR of 4-(furan-2-yl)benzaldehyde.

4-(thiophen-2-yl)benzaldehyde

^1H NMR (400 MHz, CDCl_3) δ 10.00 (s, 1H), 7.93–7.85 (m, 2H), 7.81–7.72 (m, 2H), 7.47 (dd, $J = 3.7, 1.1$ Hz, 1H), 7.40 (dd, $J = 5.1, 1.1$ Hz, 1H), 7.14 (dd, $J = 5.1, 3.7$ Hz, 1H).

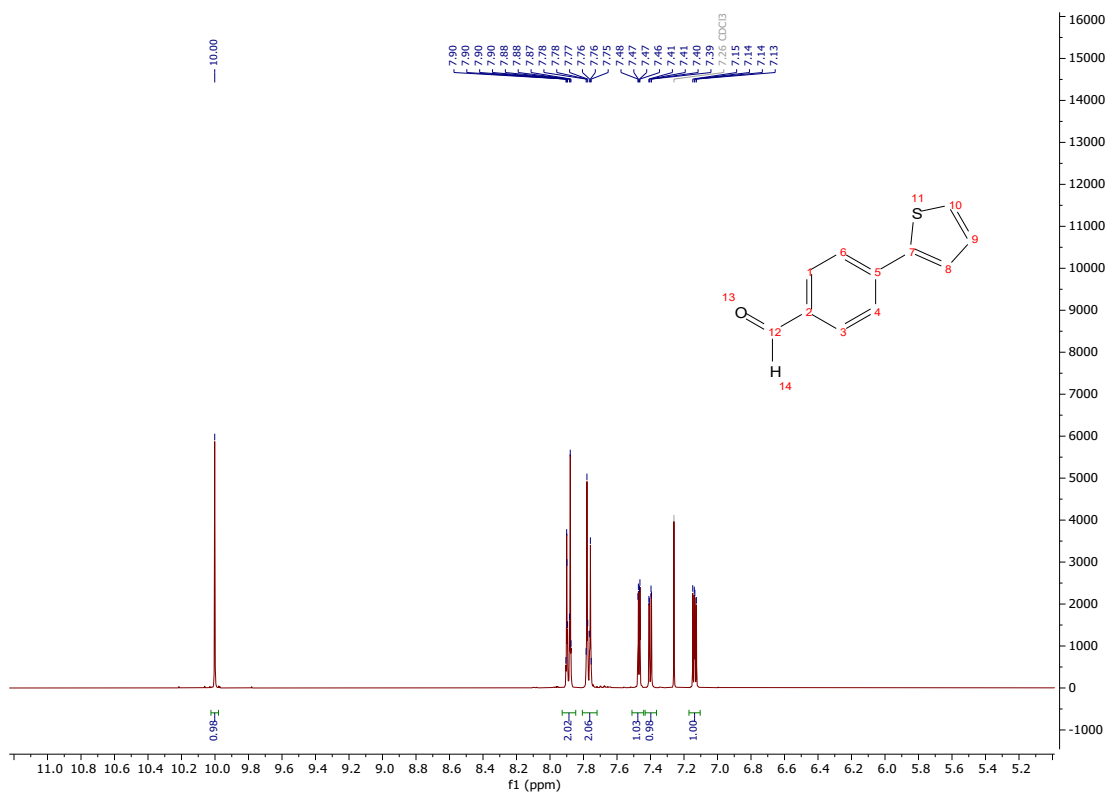


Figure S21. ^1H NMR of 4-(thiophen-2-yl)benzaldehyde.

4-methoxy-1,1'-biphenyl

^1H NMR (500 MHz, CDCl_3) δ 7.58–7.51 (m, 4H), 7.42 (t, $J = 7.5$ Hz, 2H), 7.31 (d, $J = 7.4$ Hz, 1H), 6.99 (d, $J = 8.2$ Hz, 2H), 3.86 (s, 3H).

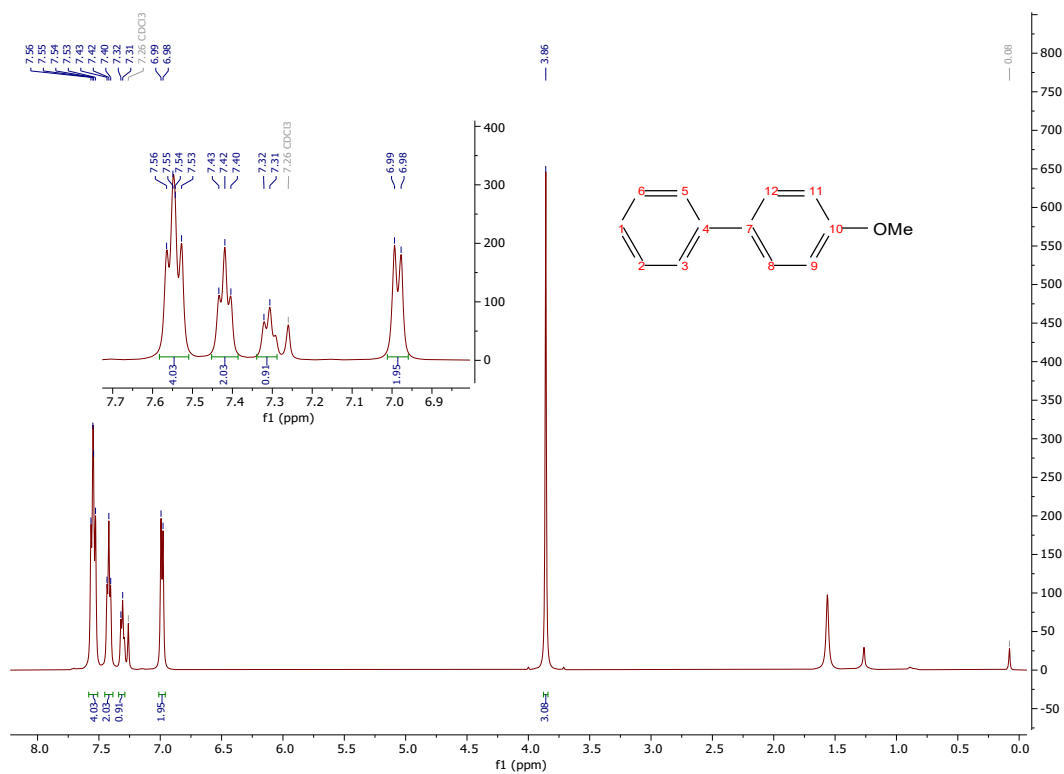


Figure S22. ^1H NMR of 4-methoxy-1,1'-biphenyl.

4-nitro-3-(trifluoromethyl)-1,1'-biphenyl

^1H NMR (500 MHz, CDCl_3) δ 8.00 (d, $J = 11.4$ Hz, 2H), 7.90 (d, $J = 8.4$ Hz, 1H), 7.62 (d, $J = 7.7$ Hz, 2H), 7.52 (dt, $J = 13.8, 7.3$ Hz, 3H).

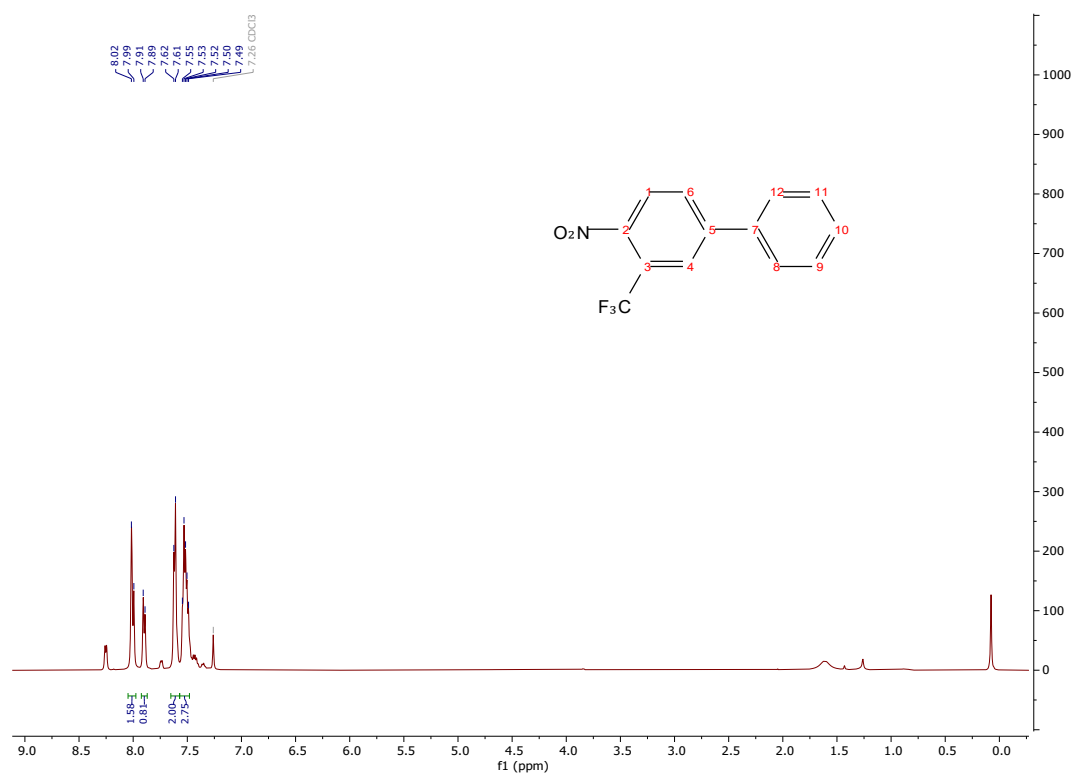


Figure S23. ^1H NMR of 4-nitro-3-(trifluoromethyl)-1,1'-biphenyl.